

Maximum Torque per Ampere Control Method for IPM Synchronous Motor based on V/f Control

Jun-ichi Itoh, Yuki Nakajima, Masakazu Kato

Dept. of Electrical, Electronics and Information Engineering

Nagaoka University of Technology

Nagaoka Niigata, Japan

itoh@vos.nagaokaut.ac.jp, nyuuki@stn.nagoakaut.ac.jp, katom@stn.nagaokaut.ac.jp

Abstract— This paper proposes a maximum torque per ampere (MTPA) control method based on V/f control for the Interior Permanent Magnetic Synchronous Motor (IPMSM). The V/f control is inherently a position sensorless method. Therefore it is simpler than the conventional methods such as the sensorless vector control method. In addition, the MTPA control can be achieved by controlling the reactive power without the information of magnet pole position. The proposed MTPA control achieves high efficiency because the copper loss can be reduced. In this paper, the proposed method is demonstrated by the by the experiments. Then, the output current can be reduced by 76 % in compared to the V/f control without MTPA. The validity of the proposed method is confirmed by experimental results.

I. INTRODUCTION

In recent years, IPMSMs have been intensively studied because of its attractive features; high efficiency, light weight and high speed rotation.

The vector control is one of the common control methods to drive the IPMSM. However, the vector control method requires a position sensor, which is composed from an encoder and a resolver, in order to detect the magnet pole position. The position sensor is one of the high cost components in an IPMSM drive system. Besides, it is difficult to put the position sensor depending on applications.

In order to not use the position sensor, many kinds of sensorless vector control methods have been studied and proposed for IPMSM [1-6]. The sensorless vector control method estimates the magnetic pole position of the IPMSM by using the motor voltage, current and motor parameters. However, the calculation for the position estimation is complicated and the decision of the control parameter in order to stabilization is difficult. In addition, the error of the position estimation occurs easily when the parameters are mismatching between the controller and motor. Especially the motor parameters will be changed by the motor temperature, flux

saturation and so on. As a result, it is difficult to certify the stability of sensorless vector control.

On the other hands, open loop control, which has no current regulator, such as V/f control methods have been studied and investigated for the IPMSM [7-9]. The V/f control method can be considered as an open loop control, because it does not require the information of the pole position. In the V/f control, the control algorithm is implemented on $\gamma\delta$ -flame where the δ -axis is corresponding to the output voltage vector of an inverter. The control algorithm is easier than that of the sensor less vector control. Especially, the motor parameters are not used in the control. In Ref [9], the MTPA ($i_d = 0$) control method based on the V/f control for Surface Permanent Magnetic Synchronous Motor (SPMSM) have proposed. However, in the IPMSM, the maximum torque per efficiency control is not achieved at $i_d = 0$ because the reluctance torque cannot be used effectively. Therefore, it is seems that the MTPA for IPMSM have not been discussed in detail.

In this paper, a MTPA control method for IPMSM based on V/f control method is proposed. The proposed method is does not need a position sensorless due to open loop control. Furthermore, the propose method can be achieved by controlling the reactive power to regulate with the current phase.

This paper is organized as follows; first the principle of the V/f control is introduced. Next, MTPA for IPMSM is proposed. After that, the MTPA control method based on V/f control method is confirmed by simulation. In the simulation, it is confirmed that the output current in dq-frame can be corresponded to the MTPA operation point. Furthermore, The proposed MTPA is demonstrated in the experiment using a 1.5-kW IPMSM with a 2-level inverter. As a result, the proposed MTPA reduces the output current by nearly 76 % compared to not use MTPA.

II. V/F CONTROL BASED ON THE OUTPUT VOLTAGE VECTOR OF THE INVERTER

A. Basic Principle

Fig. 1 shows the relationship between $\gamma\delta$ -frame and dq-frame. Generally, in the dq-frame of the IPMSM control, the d-axis is defined as the direction of the flux vector by the permanent magnet and the direction of the q-axis is defined as the electromotive force vector. Therefore, it is very important to identify the flux vector in the vector control. However, the V/f control method is implemented on the $\gamma\delta$ -frame, and the δ -axis is defined as the direction of the output voltage vector of the inverter. Therefore, the δ -axis means active power component and the γ -axis means reactive power component.

The voltage equation of IPMSM based on dq-frame is given by (1).

$$\begin{bmatrix} v_d \\ v_q \end{bmatrix} = \begin{bmatrix} R_a + pL_d & -\omega_{re}L_q \\ \omega_{re}L_d & R_a + pL_q \end{bmatrix} \begin{bmatrix} i_d \\ i_q \end{bmatrix} + \begin{bmatrix} 0 \\ \omega_{re}\psi_m \end{bmatrix} \quad (1)$$

where $v_{d(q)}$ is the d(q)-axis voltage, $i_{d(q)}$ is the d(q)-axis current, ω_{re} is the electric angular frequency, p is the differential operator, R_a is the armature resistance, $L_{d(q)}$ is the d(q)-axis synchronous inductance, and ψ_m is the flux linkage of the permanent magnet. Then, the voltage equation of IPMSM based on $\gamma\delta$ -frame is obtained by (2).

$$\begin{bmatrix} v_\gamma \\ v_\delta \end{bmatrix} = \begin{bmatrix} R_a + pL_d & -\omega_l L_q \\ \omega_l L_d & R_a + pL_q \end{bmatrix} \begin{bmatrix} i_\gamma \\ i_\delta \end{bmatrix} + \omega_{re}\psi_m \begin{bmatrix} \sin\theta \\ \cos\theta \end{bmatrix} \quad (2)$$

where $v_{\gamma(\delta)}$ is the $\gamma(\delta)$ -axis voltage, $i_{\gamma(\delta)}$ is the $\gamma(\delta)$ -axis current, and ω_l is the rotating speed of $\gamma\delta$ -frame. Here, the equation of the torque and the relationship (ignored the viscosity resistance) between the electric angular velocity and the torque on $\gamma\delta$ -frame is given by (3) and (4), respectively.

$$T = P_f \psi_m i_q = P_f \psi_m (i_\gamma \sin\theta + i_\delta \cos\theta) \quad (3)$$

$$p\omega_{re} = \frac{P_f (T - T_L)}{J} \quad (4)$$

where P_f is the pairs of poles, T is the output torque, T_L is the load torque, and J is the inertia of the motor. The gap angular θ between $\gamma\delta$ -frame and dq-frame is given by

$$p\theta = \omega_l - \omega_{re} \quad (5)$$

In the steady state, the rotating speed in either the $\gamma\delta$ -frame or the dq-frame is the same value. However, in transient state, the gap angular between $\gamma\delta$ -frame and dq-frame occurs due to the differential in the rotating speed. Here, the differentiation of θ is equaled to the difference between ω_l and ω_{re} .

From the definition of the $\gamma\delta$ -frame, the output voltage vector v_δ is given in the δ -axis. In addition, the electromotive force $\omega_{re}\psi_m$ occurs on the q-axis. Therefore, the gap angular θ between the γ -axis and dq-frame is subjected to the load angular.

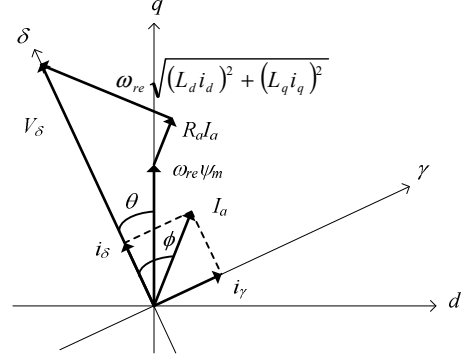


Fig. 1. Relationship between $\gamma\delta$ -frame and dq-frame. The δ -axis is defined as the direction of the output voltage vector of the inverter, and the direction of the q-axis is defined as the electromotive force vector.

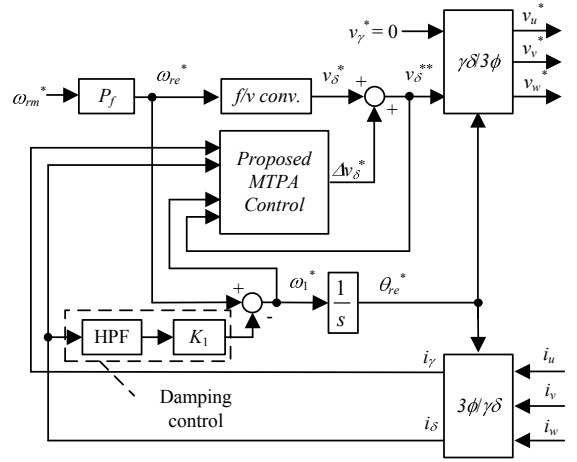


Fig. 2. V/f control method based on $\gamma\delta$ -frame. The motor is controlled by V/f control method with damping control.

B. Damping Control

Fig. 2 shows the block diagram of the V/f control method based on $\gamma\delta$ -frame. When a motor is controlled by simple V/f control method which means an open loop control, the torque vibration is generated due to the resonance between the synchronous the reactance and the moment of inertia of the IPMSM as indicated in Ref. [9].

In Ref. [9], the V/f control method based on $\gamma\delta$ -frame with damping control was proposed. The torque vibration causes the vibration of the δ -axis current because the δ -axis current is active current. In another words, the vibration component of the δ -axis current can assume the vibration component of the torque. The damping control suppresses the torque vibration with feedback the δ -axis current into the electric angular frequency reference value ω_{re}^* in order to cancel the load angular vibration. When the damping control is applied, the damping coefficient is a function to the feedback gain K_1 , therefore, the stable operation can be achieved.

III. MAXIMUM TORQUE AMPERE CONTROL METHOD BASED ON V/F CONTROL

MTPA ($i_d = 0$) control can achieve high efficiency for the SPMSM. On the other hands, the MTPA is not achieved at $i_d =$

0 in of IPMSM due to the reluctance torque. Therefore, in this chapter, MTPA control based on V/f control for IPMSM is discussed. In order to achieve the MTPA in IPMSM, the reactive power is used.

The reactive power Q_{dq} on dq-frame is given by (6)

$$Q_{dq} = v_q i_d - v_d i_q \quad (6)$$

By substituting (1) into (6), the reactive power Q_{dq} can be expressed as (7).

$$Q_{dq} = \omega_{re} \{L_d i_d^2 + L_q i_q^2 + \psi_m i_d\} \quad (7)$$

Equation (7) can be re-written as (8) by using I_a and β .

$$Q_{dq} = \omega_{re} \{L_d I_a^2 \sin^2 \beta + L_q I_a^2 \cos^2 \beta - \psi_m I_a \sin \beta\} \quad (8)$$

where the equation of the current phase β when the MTPA control [10] is given by

$$\beta = \sin^{-1} \left(-\frac{\psi_m}{4(L_q - L_d)I_a} + \sqrt{\left(\frac{\psi_m}{4(L_q - L_d)I_a}\right)^2 + \frac{1}{2}} \right) \quad (9)$$

Note that the current phase β becomes zero when L_d equal to L_q i.e. it means SPMSM because 1st term equals to 2nd term. If it is defined as $I_a \sin(\beta) = X$, then the equation of the reactive power is obtained by

$$Q_{dq} = \omega_{re} \{L_d X^2 + L_q (I_a^2 - X^2) - \psi_m X\} \quad (10)$$

Equation (10) is the reactive power when the MTPA control is achieved. On the other hands, the reactive power based on $\gamma\delta$ -frame $Q_{\gamma\delta}$ is given by

$$Q_{\gamma\delta} = v_\delta i_\gamma \quad (11)$$

If the $Q_{\gamma\delta}$ as shown in (11) equals to Q_{dq} as shown in (10), the MTPA control can be achieved. In another words, the satisfaction of (12) achieve the MTPA control during the V/f control.

$$\omega_{re} \{L_d X^2 + L_q (i_\gamma^2 + i_\delta^2 - X^2) - \psi_m X\} = v_\delta i_\gamma \quad (12)$$

In order to satisfy the condition in (12), the PI controller is implemented to regulate the δ -axis voltage v_δ .

Fig. 3 show the control block diagram of the proposed MTPA control method. The control block shown in Fig. 3 is same as the proposed MTPA control block shown in Fig. 2. In addition, Q_{dq} command value is calculated from (10) at the Q_{dq}^* calc. block in Fig. 3. The proposed MTPA block conform $Q_{\gamma\delta}$ to Q_{dq}^* by PI controller. The PI controller outputs the δ -axis voltage command compensation value of Δv_δ^* . The Δv_δ^* compensate the δ -axis voltage command v_δ^* in order to accomplish (12).

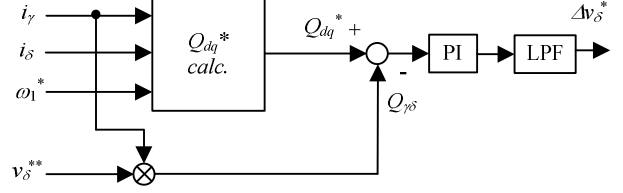


Fig.3 High Efficiency control method for IPMSM. Q_{dq} command value is calculated from (10) at the Q_{dq}^* calc. block
Table.1 Motor Parameters used in simulations. The IPMSM has a saliency ratio of 2.0 and the rated power is 1.5 kW

Motor Power	1.5kW
Rated Current	6.1A _{rms}
Rated Speed	1800rpm
Number of Poles	6poles
Winding Resistance	0.783Ω
d-axis Inductance	11.5mH
q-axis Inductance	23.0mH
Interlinkage magnetic flux	0.246V·s/rad

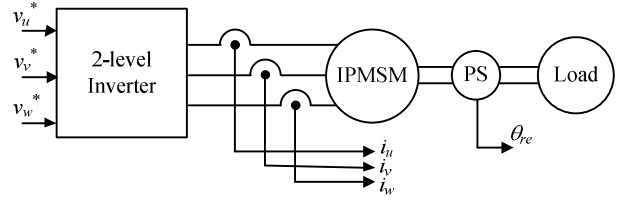


Fig.4 Simulation model. The load is a constant torque load.

IV. SIMULATION RESULTS

In order to confirm the operation, the proposed method is simulated in PLECS (*Plexim GmbH*). Table 1 shows the motor parameters, and the IPMSM has a saliency ratio of 2.0 and the rated power is 1.5 kW. In addition, the switching frequency is 10 kHz.

The simulation model uses a 2-level inverter as shown in Fig. 4. Note that the dq-frame current is calculated from the inverter output current by using the information of the magnet pole position in order to the confirming of the MTPA operation. However, the information of the magnet pole position is not required in the actual IPMSM system due to open loop. In addition, the load is a constant torque load.

The voltage command v_δ^* in the V/f control is calculated by (13).

$$v_\delta^* = vf(1 - v_{bst})\omega_{re}^* + v_{bst} \quad (13)$$

where vf is the V/f ratio and v_{bst} is the torque boost voltage which compensates the voltage drop at the armature resistance. The V/f ratio is defined as the ratio, where the output voltage is proportional to the motor frequency. The V/f ratio is defined as 1, where 90 Hz is equivalent to 180 V in this paper. The torque boost voltage is 0.05 p.u. of the rated voltage (180 V) that is equal to the percentage of R_a .

Fig. 5 shows the waveforms at the d and q-axis current, output current and d-axis voltage command with the proposed MTPA method. The operation point in the simulation are as follows; the rotating speed command is 0.2 p.u. and the load torque is 0.2 p.u.. The V/f control with the damping control is

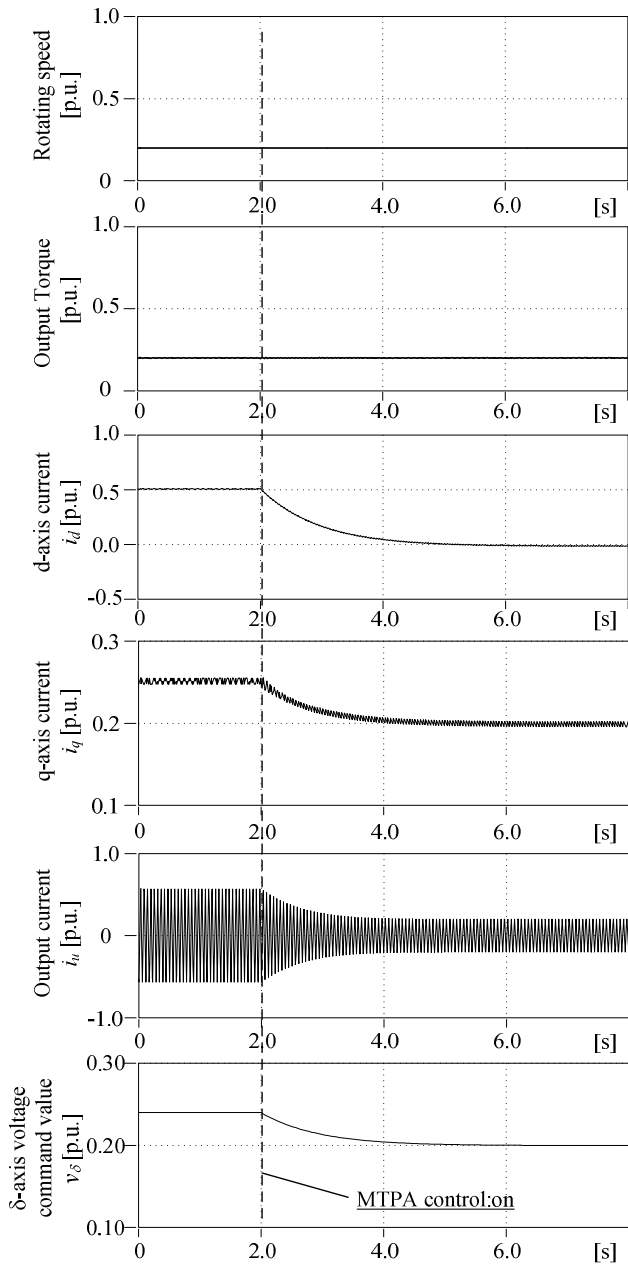


Fig. 5 Operation of MTPA control method based on V/f control (Load Torque is 0.2 p.u. and Rotation speed is 0.2 p.u.). The amplitude of the output current is reduced from 0.57 p.u. to 0.20 p.u. with proposed MTPA control.

applied from 0 s to 2.0 s, and then the V/f control and the MTPA control (including the damping control) is applied from 2.0 s and onwards.

The d and q-axis currents decrease when the MTPA control is applied because the δ -axis voltage command value is compensated by the high efficiency control system as shown in Fig. 2. The q-axis current decreasing cause the magnet torque decreasing. Note that the output torque remains unchanged even d and q-axis current have changed. Therefore, the reluctance torque compensates for the magnet torque decreasing. In addition, the amplitude of the output current is

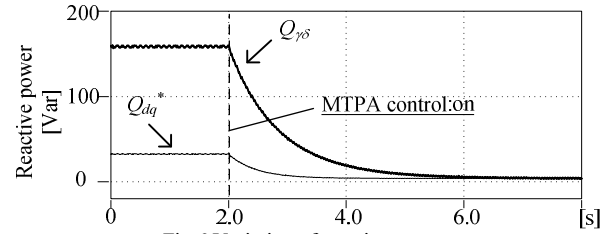


Fig. 6 Variation of reactive power (Load Torque is 0.2 p.u. and Rotation speed is 0.2 p.u.). The reactive power $Q_{\gamma\delta}$ becomes converged as the command Q_{dq}^* .

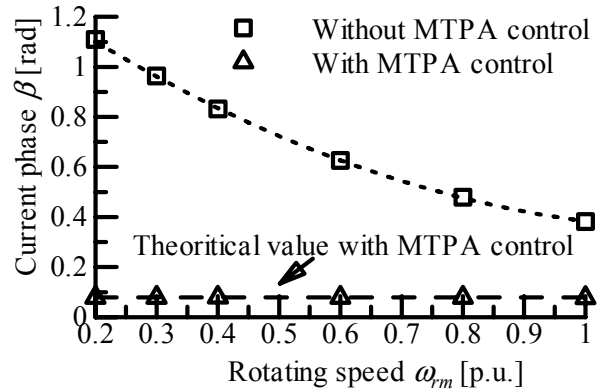


Fig. 7 Variations of Current phase with/without MTPA control method (Load torques are 0.2 p.u.). In the case the MTPA control is applied, the current phase is corresponded to the theoretical current phase that can achieve the MTPA control operation.

reduced from 0.57 p.u. to 0.20 p.u. The effectiveness of the proposed method is demonstrated in the simulation result.

In addition, the d-axis current is -0.016 p.u. and the q-axis current is 0.199 p.u. at the time 6.0 s. Therefore, the current phase β is 0.08 rad. and this value is equivalent to the β , which is calculated from (9). Therefore, it is confirmed that the MTPA control can be achieved.

Fig. 6 shows the relationship between the reactive power command value Q_{dq}^* and the detected value $Q_{\gamma\delta}$ when the MTPA control is applied. The operation point is similar to Fig. 5. The reactive power becomes converged as the command has decrease because the PI control is implemented. Therefore, it is confirmed that the regulation of the reactive power can be achieved.

Fig. 7 shows the differences in the current phase between the case with and without applying the MTPA control. The operation points are as follows: the rotating speed is from 0.2 p.u. to 1.0 p.u. and the output torque is 0.2 p.u. constantly. Without the MTPA control, the current phase varies in subjected to the load condition, due to the difference in the load angular. In addition, the current phase is different from the theoretical current phase that can achieve the MTPA control operation. Therefore, the V/f control method without the MTPA control cannot control the reluctance torque. On the other hands, in the case the MTPA control is applied, the current phase is corresponded to the theoretical current phase that can achieve the MTPA control operation. Thus, the reluctance torque can achieve its maximum by applying the proposed method.

Fig. 8 shows the current phase of the theoretical value and simulation result when the MTPA control is applying. The operation point is as follows: the rotating speed and output torque are varied from 0.2 p.u. to 1.0 p.u. respectively. As the result, at all of the simulation conditions, the theoretical results are almost identical to the simulation results. It is confirmed that the proposed method can achieve the MTPA control at various kind of load conditions.

Fig. 9 shows the decreasing rate of the output current with the proposed MTPA. Here, the percentage is represented in a form that, $100\% - (I_a \text{ (with MTPA)} / I_a \text{ (without MTPA)})$, and therefore the larger the percentage means that the output current can be reduced largely. At the operation point of the rotating speed and output torque are 0.2 p.u., the output current is reduced by more than 60%. The effectiveness of the proposed method and its characteristics are demonstrated under various speed conditions.

V. EXPERIMENTAL RESULTS

Fig. 10 shows the schematic of the experimental system. The IPMSM is driven by a 2-level inverter and the switching frequency is 10 kHz. In addition, the load motor is used as load machine to supply a constant torque. In this experiment, in order to confirm the effectiveness of the proposed MTPA control, the dq-frame current is calculated from the inverter output current using the information of magnet pole position which is obtained from Hall Effect sensor. However, the information of magnet pole position is not used in the actual motor drive system. In addition, the motor parameters in shown Table 1.

Fig. 11 shows the experimental result of the IPMSM drive operation using a 2-level inverter with the MTPA control method based on the V/f control method. The experimental conditions are follows; the rotating speed command is 0.4 p.u. and the load torque is 0.2 p.u.. From Fig. 13, the output current can be reduced by 68 % (from 0.72 p.u. to 0.23 p.u.) after applying the MTPA control method. If the proposed MTPA control is disabled, the reluctance torque cannot reach its maximum and the output current becomes large. On the other hands, if the proposed MTPA control is enabled, the reluctance torque can reach its maximum and the output current becomes its minimum.

Fig. 12 shows the step response waveform with the MTPA control method based on the V/f control method. The rotating speed is 0.2 p.u.. At the 0.8 s, the load torque is varied from 0.2 p.u. to 0.4 p.u.. When the output torque increases, the output current increases due to the increasing the load power. In addition, the d-axis current decreases and the output current increases. It means that the current phase β is varied due to the variation of the output current amplitude I_a in (9). Furthermore, it is confirmed that the proposed MTPA control is stable against the step load variation.

Fig. 13 compares the amplitude of the output current when the reactive power is varied by adding the error Q_{dqref_vary} as (14).

$$Q_{dq}^* = Q_{dqref_vary} + \omega_{re} \{L_d X^2 + L_q (I_a^2 - X^2) - \psi_m X\} \quad (14)$$

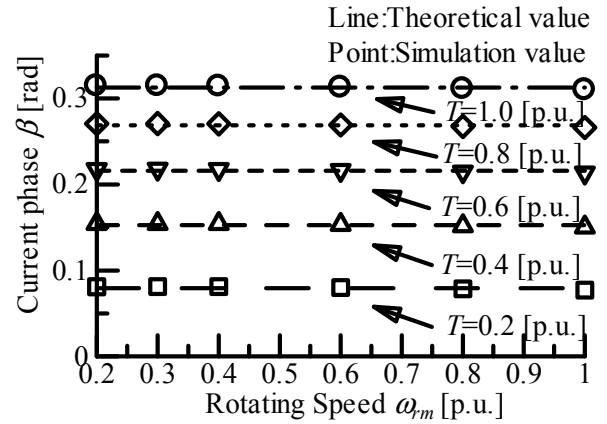


Fig.8 Comparison of current phase between simulation results and ideal values. The theoretical results are almost identical to the simulation results.

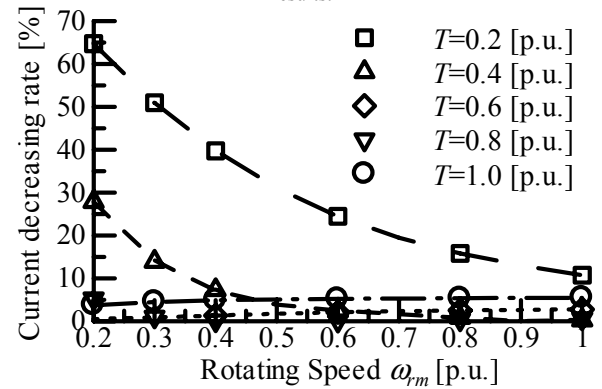


Fig.9 Current decreasing rates with MTPA control. The percentage is represented in a form that, $100\% - (I_a \text{ (with MTPA)} / I_a \text{ (without MTPA)})$.

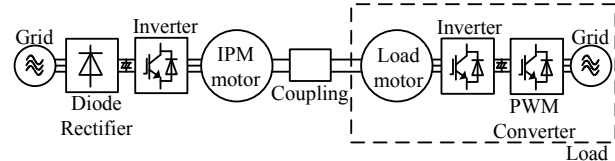


Fig.10 Experimental system. The IPMSM is driven by a 2-level inverter and the switching frequency is 10 kHz.

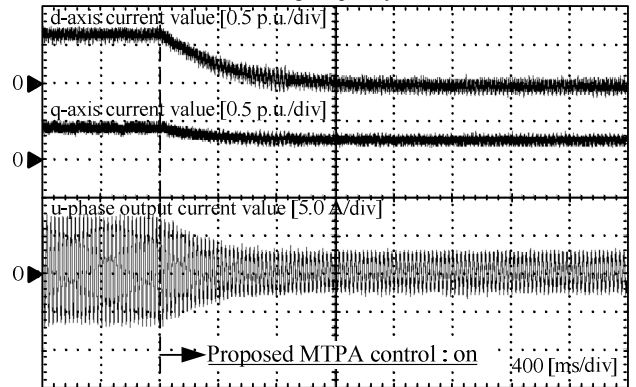


Fig.11 Experimental results (load torque is 0.2 p.u. and rotating speed is 0.4 p.u.). The output current can be reduced by 68 % (from 0.72 p.u. to 0.23 p.u.) after applying the MTPA control method.

In the Fig. 13, the horizontal axis shows the difference between the reactive power command and the theoretical

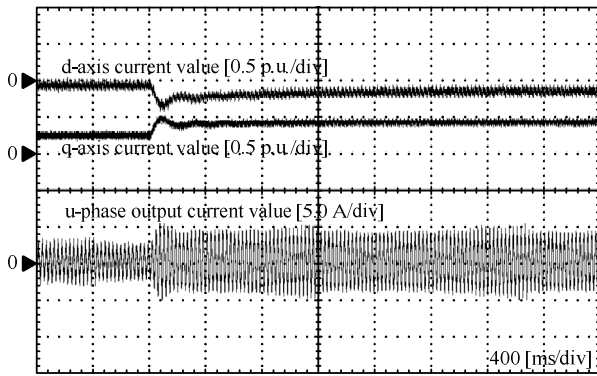


Fig. 12 Experimental results (load torque is from 0.2 p.u. to 0.4 p.u. at 0.8 s, and rotating speed is 0.4p.u.). It is confirmed that the proposed MTPA control is stable against the step load variation.

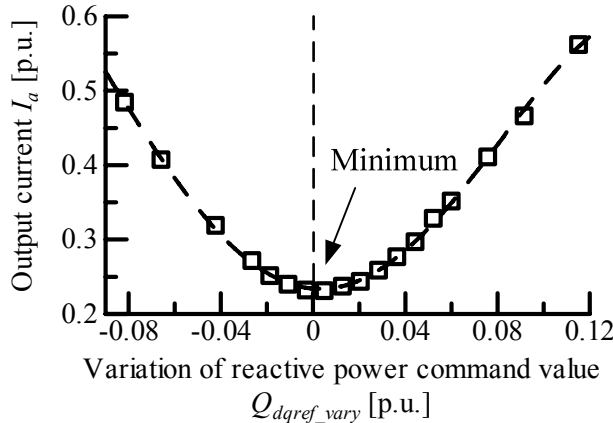


Fig.13 Relationship between Q_{dqref} and I_a (load torques are 0.2 p.u. and rotating speeds are 0.2 p.u.). It is confirmed that the amplitude of the output current becomes minimum at 0.23 p.u. when the reactive power command value is equivalent to the theoretical value.

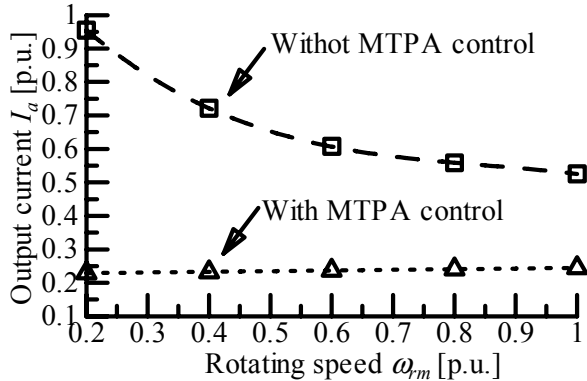


Fig.14 Variation of output current with/without MTPA control method (Load torques are 0.2 p.u.). Even if the load condition is varying, the proposed method can reduce the output current.

value Q_{dqref} . From Fig. 5, it is confirmed that the amplitude of the output current becomes minimum at 0.23 p.u. when the reactive power command value is equivalent to the theoretical value. It means that the reactive power command from (10) can minimize the output current at the constant load torque.

As a result, the effectiveness of the proposed MTPA method can be observed.

Fig. 14 shows the amplitude of output current when the load condition is varied. From the Fig. 15, even if the load condition is varying, the proposed method can reduce the output current. In addition, the output current can be reduced by 76 % (from 0.96 p.u. to 0.23 p.u.).

VI. CONCLUSIONS

This paper proposed a maximum torque per ampere (MTPA) control method based on the V/f control and the validity of the proposed method was confirmed by experimental results. The magnet pole position information is not necessary because the proposed method uses the reactive power control which is calculated on $\gamma\delta$ -frame. From the experimental result, it is confirmed that the output current can be reduced by 76 % compared to not use the proposed MTPA.

REFERENCES

- [1] M. J. Corley, and R. D. Lorenz, "Rotor Position and Velocity Estimation for a Salient-Pole Permanent Magnet Synchronous Machine at Standstill and High Speeds", IEEE Transactions on Industry Applications, vol. 34, no. 4, pp. 784-789, 1998
- [2] S. Morimoto, K. Kawamoto, M. Sanada, Y. Takeda, "Sensorless control strategy for salient-pole PMSM based on extended EMF in rotating reference frame", IEEE Transactions on Industry Applications, vol. 38, no. 4, pp. 1054-1061, 2002.
- [3] Zhiqian Chen, M. Tomita, S. Dok i, S. Okuma, "An extended electromotive force model for sensorless control of interior permanent-magnet synchronous motors", IEEE Transactions on Industrial Electronics, vol. 50, no. 2, pp. 288-295, 2003.
- [4] S. Ogasawara, H. Akagi, "Implementation and position control performance of a position-sensorless IPM motor drive system based on magnetic saliency", IEEE Transactions on Industry Applications, vol. 34, no. 4, pp. 806-812, 1998.
- [5] T. Noguchi, S. Kohno, "Mechanical-Sensorless Permanent-Magnet Motor Drive Using Relative Phase Information of Harmonic Currents Caused by Frequency-Modulated Three-Phase PWM Carriers", IEEE Transactions on Industry Applications, vol. 39, no. 4, pp. 1085-1092, 2003.
- [6] M. Hasegawa, S. Yoshioka, K. Matsui, "Position Sensorless Control of Interior Permanent Magnet Synchronous Motors Using Unknown Input Observer for High-Speed Drives", IEEE Transactions on Industry Applications, vol. 45, no. 3, pp. 938-946, 2009.
- [7] K. Kaku, N. Yamamura, Y. Tanehiro, "A Novel Technique for a DC Brushless Motor Having No Position Sensors", IEEJ Trans. D, vol. 111, no. 8, pp. 639-644, 1991.
- [8] H. Urita, N. Yamamura, Y. Tanehiro, "On General Purpose Inverter for Synchronous Motor Drive", IEEJ Trans. D, vol. 119, no. 5, pp. 707-712, 1999.
- [9] J. Itoh, N. Nomura, H. Ohsawa, "A Comparison between V/f Control and Position-Sensorless Vector Control for the Permanent Magnet Synchronous Motor", Proc. of the Power Conversion Conference PCC Osaka 2002, Vol. 3, pp. 1310-1315, 2002.
- [10] S. Morimoto, Y. Takeda, K. Hatanaka, Y. Tong, T. Hirasa, "Design and control system of inverter-driven permanent magnet synchronous motors for high torque operation", IEEE Transactions on Industry Applications, vol. 29, no. 6, pp. 1150-1155, 1993